Title: Loading of alkaline hydroxide nanoparticles on the
surface of Fe_2O_3 for the promotion of photocatalytic activity

Authors: M. Khajeh Aminian, S.K. Fatah

PII: S1010-6030(18)31264-4
DOI: https://doi.org/10.1016/j.jphotochem.2019.01.003
Reference: JPC 11662

To appear in: *Journal of Photochemistry and Photobiology A: Chemistry*

Received date: 31 August 2018
Revised date: 3 January 2019
Accepted date: 4 January 2019

Please cite this article as: Aminian MK-ErrorvCtInIinicfImhlt6c/̈>, Fatah SK, Loading of alkaline hydroxide nanoparticles on the surface of Fe_2O_3 for the promotion of photocatalytic activity, *Journal of Photochemistry and amp; Photobiology, A: Chemistry* (2019), https://doi.org/10.1016/j.jphotochem.2019.01.003

Loading of alkaline hydroxide nanoparticles on the surface of Fe_2O_3 for the promotion of photocatalytic activity

M. Khajeh Aminian[1], S. K. Fatah[1,2]*

[1]Department of Physics, Yazd University, Yazd, Iran.

[2]Department of Physics, University of Garmian, Kalar, KRG, Iraq.

*Corresponding Author: kh.aminian@yazd.ac.ir

Highlights

- Iron oxide (Fe_2O_3) and iron oxide hybrid based materials have attracted attention as a photocatalyst.
- A new photocatalyst system is designed based on loading of alkaline hydroxide nanoparticles on Fe_2O_3 which is sensitive to visible light.
- This photocatalyst system is based on charge transfer between Fe_2O_3 as a supporter material and several alkaline oxide materials as a cocatalyst.
- The photocatalytic evaluation reveals that the new system promotes the photoactivity of Fe_2O_3 under visible light irradiation.

Abstract

This study focused on surface modification of iron oxide (Fe_2O_3) by loading alkaline oxide nanoparticles to investigate the effect of surface interactions on photocatalytic activity of this material. Fe_2O_3 was loaded by NaOH, KOH, and CsOH, with 0.05, 0.1, 0.4, and 1 wt% by impregnation method. The photocatalytic evaluation was carried out in a gas phase for degradation of Iso-Propyl alcohol (IPA) to acetone. The prepared samples were characterized by X-ray diffraction, UV-Visible diffuse reflectance spectroscopy, and scanning electron microscopy SEM. The photocatalytic evaluation resulted the photoactivity of Fe_2O_3 increases to an optimum extent by loading of alkaline hydroxides on the surface. The enhancement of photoactivity of Fe_2O_3 after loading can be attributed to the surface chemical reactions and transfer of photogenerated electrons from the conduction band of Fe_2O_3 to alkaline nanoparticles. Also, multi-electron oxygen reduction is another way supposed to facilitate the photocatalytic reaction.

Keywords: Fe_2O_3, KOH, NaOH, CsOH, Photocatalysis, Photodegradation, Impregnation.

1. Introduction

Many harmful organic pollutants exist in the air, water and soil environments extensively [1]. Most of the organic pollutants can be degraded on the surface of photocatalyst materials under solar illumination in the natural environment [2-5]. The conventional photocatalysts such as TiO_2 [6-9], ZnO [9,10] and WO_3 [11-15] have a wide band gap and therefore they are limited in the absorption of solar energy to less than ~ 4%. Thus, their low material cost would be overshadowed by the expense of enormous area structures required for the solar exposure in an environmental application. Among the inexpensive metal oxides absorb visible-light illumination; iron oxide and iron oxide hybrid based materials have attracted attention as a potential photocatalyst because of its stability, safety and low cost [4, 15-21]. In addition, Fe_2O_3 (Hematite) has the advantage that its band gap is ~2 eV allowing for absorption of 40% of the solar spectrum [9,22,23]. Despite the seemingly favorable characteristics of Hematite, some factors limit its performance. The maximum solar to chemical efficiency reported is less than 3% under AM 1.5 illumination [16]. The low efficiency may be a result of these factors: (1) low electron mobility (~0.1 $cm^2V^{-1}S^{-1}$) [18, 24, 25], which reduces the electron collection efficiency, (2) high electron-hole recombination rates [9, 21,22,23,26, 27], (3) high conduction band energy potential (~0.2 V vs NHE), and (4) anisotropic conductivity, which is 4 orders of magnitude higher within the [001] plane than parallel to [001] [25, 28-30].

To enhance the photoactivity of Fe_2O_3, it needs to think about the mentioned challenges above. Recombination in low mobility materials can be minimized by decreasing the particle size to less than the minority carrier diffusion length [31]; for Fe_2O_3-Hematite, the hole diffusion length was reported less than 20 nm [32-34]. Therefore, fabrication of Fe_2O_3-Hematite nanostructures is a way to enhance the photoactivity of it [23]. Grätzel and his colleagues have reported a high water photooxidation property by dendritic Fe_2O_3 nanostructures having a feature size of 10 to 20 nm at the surface [35]. The surface of this material was treated with $Co(NO_3)_2$ solution to load a monolayer of Co atoms on the surface. Water photooxidation efficiency of this material was promoted by loading of Co atoms on the surface. Recently water photooxidation was investigated by Fe_2O_3 nanoparticles embedded in clay compound (Na^+ treated Montmorillonite) [36]. The efficiency of photooxidation increased with the loaded photocatalyst until the loading amount reached ca. 3 wt%, and decreased in the larger loading amount.

High recombination rate and high conduction band energy potential of Fe_2O_3 can be influenced simultaneously by loading of a relevant material on the surface of Fe_2O_3. Loading of a relevant material on the surface of Fe_2O_3 may cause transfer of photogenerated electrons from conduction band (CB) of Fe_2O_3 to energy levels of this new material as it has been already reported for different materials [37-39]. This phenomenon reduces the electron-hole recombination rate in Fe_2O_3. In addition, the transferred photoelectrons can be excited to a lower energy potential by absorption of new energy photons.

On the basis of this background, we designed a new photocatalyst system sensitive to visible light. This photocatalyst system is based on charge transfer between Fe_2O_3 as a supporter material and several alkaline oxide materials as cocatalysts. The photocatalytic evaluation shows that the new system promotes the photoactivity under visible light irradiation.

2. Experimental Methods

Three different photocatalyst systems of alkaline oxide/Fe_2O_3 were prepared by impregnation method. 100 mg of NaOH, KOH, and CsOH from (Wako corp.) were dissolved in 100 g of distilled water separately. Four samples of 1.0 g commercial Fe_2O_3-Hematite (Wako corp., BET surface area 5.2 m^2 g^{-1}) were mixed with 0.3, 0.5, 0.7 and 1 ml NaOH solution separately. The mixtures were dried on a hot plate and heated at 450 °C for 2h. Loading of KOH and CsOH on Fe_2O_3 were performed in the same procedure.

The photocatalytic evaluation was carried out in a cylindrical air-filled static pyrex glass vessel (500 ml of total volume) for degradation of isopropyl alcohol (IPA) to acetone. The catalyst powders (~0.6 g) were evenly dispersed on the bottom of a circular glass dish to have a uniform area of ~8 cm^2 and the dish was mounted in the vessel. The vessel was filled with artificial pure air to replace the CO_2-containing natural air. After injection of IPA and prior to light irradiation, the vessel was kept in the dark for one hour to get adsorption saturation of IPA on the sample surface. Upon light irradiation, gaseous sample (0.5 ml) was periodically extracted from the reaction vessel and measured on a gas chromatograph (GC-14B, Shimadzu) equipped with a flame ionization detector (FID) for analysis of IPA/acetone. The light source was a 300 W xenon arc lamp (ILC Technology, CERMAX LX-300). A cutoff filter (L44, Hoya Optics) was used to obtain visible light ($\lambda > 440$ nm). UV–visible diffuse reflectance spectrum was measured on a UV–visible spectrometer (UV-2500, Shimadzu) at room temperature. A field emission scanning electron microscope (FE-SEM, JEOL-JSM 6500F) was used for morphology observation and X-ray diffractometer (XRD, X'pert Pro;

PANalytical Co., Netherlands) was used for determining the crystallization properties of samples.

3. Results and Discussion

IPA decomposition is a standard reaction for photocatalytic activity evaluation [27]. In the beginning, the IPA decomposition should be evaluated into acetone by photogenerated holes at the initial reaction stage [27,40]. In figure 1-a the results of the generated acetone in the photodegradation process of IPA on the surface of iron oxide (Fe_2O_3) by loading nanoparticles of sodium hydroxide (NaOH) has been demonstrated. The figure detailed on the different amount of NaOH has been used on the surface of Fe_2O_3 with the amounts of 0.06 wt%, 0.1 wt%, 0.4 wt% and pure Fe_2O_3. All the samples were heated for 2 h at 450 ^{0}C. It can be noticed from the figure, the samples with the 0.06 wt% and 0.1 wt% of NaOH can improve the photoactivity of Fe_2O_3 surface more than samples of 0.4 wt% by increasing acetone concentration in the reaction. The highest value of acetone concentration was obtained by sample 0.06 wt%, which is more than 2 times higher than that of the pure Fe_2O_3 sample.

In order to understand more about surface modification of Fe_2O_3 with the loading of alkaline hydroxides, various samples were loaded by KOH and CsOH with the same method of NaOH samples. Figure 1-b indicates the acetone generation during the process of photodegradation of IPA reaction on the surface of Fe_2O_3 with different amounts of 0.05, 0.1 and 0.4 wt% KOH loading. Figure 1-c indicates the same plots with amounts of 0.05, 0.1, 0.3 and 1 wt% of CsOH loading. It can be observed from both figures, the samples with 0.05 and 0.1 wt have the highest photoactivity and they enhanced the photoactivity of Fe_2O_3 3 times than that of the pure one. While, 0.4 wt% of both alkaline hydroxides have decreased the degradation of acetone concentration compared to the pure one, due to the photocatalytic activity of iron oxide declined. Notably speaking from figure 1-a, 1-b and 1-c loading of alkaline hydroxides NaOH, KOH, and CsOH have a similar effect on the photoactivity of

Fe_2O_3. However, the samples loaded with KOH are more reactive than that of NaOH and CsOH, means KOH can enhance the photoactivity the most. It can be observed in figure 2. This result has corresponded to the same effect which published earlier about WO_3 surface modification [39]. A chemical property is not the only reason for the enhancement of photoactivity, but also the photoreduction and photooxidation is the reason in the process.

After the acetone generation under the irradiation of visible light, the next process was CO_2 generation due to further visible light irradiation. This step of CO_2 generation can be described as the final process of photocatalytic reaction on the surface of alkaline loaded Fe_2O_3 [27]. In figure 3 CO_2 generated under visible light irradiation for different samples with amounts of 0.05 wt%, 0.1 wt%, 0.4 wt% of KOH and the pure sample of Fe_2O_3 can be seen. According to the figure, all samples loaded with KOH have enhanced the photocatalytic properties of Fe_2O_3 more than that of the pure sample.

The surface area of 0.05 wt% KOH/Fe_2O_3 was measured by BET analysis about 5.5 $m^2\ g^{-1}$. It can be observed that it is not so different from the origin pure sample (5.2 $m^2\ g^{-1}$).

The scanning electron microscopy (SEM) images of Fe_2O_3 samples loaded with alkaline nanoparticles can be seen in figure 4. Figure 4-a shows SEM of NaOH/Fe_2O_3 sample. Some small particles of NaOH or maybe Na_2O, having a size less than 20 nm, have covered the surface of Fe_2O_3. Similarly, this case can be observed in figure 4-b for the sample of KOH/Fe_2O_3 with some nanoparticles with the size less than 20 nm on the surface. However, CsOH on the surface of Fe_2O_3 has formed a bit differently, in figure 4-c can be noticed that the small sphere-like particles formed on the surface of Fe_2O_3 which they agglomerated in some places and made particles with the size between 10-50 nm. The morphology of pure Fe_2O_3 sample is observed in figure 4-d. It shows the same structure as 4-a, 4-b, and 4-c except for the number of small particles on the surface. It can be concluded that the small particles do not belong to the Fe_2O_3 structure. The histogram of particle size for pure Fe_2O_3 and 0.05 wt%

KOH/Fe_2O_3 was plotted in fig. 5. The average particle size for pure Fe_2O_3 and 0.05 wt% KOH/Fe_2O_3 are 106 and 116 nm respectively. It shows the average particle size does not change so much after KOH modification. This might be due to the loss of water during reaction between KOH and Fe_2O_3 surfaces, this reaction has been explained in reaction (2) in the next sections.

After photocatalytic process, the SEM images of Fe_2O_3 loaded alkaline nanoparticles have been shown in fig. 6. Comparing to fig. 4, it can be observed that the morphology is approximately same as that of the samples before photocatalytic reaction.

FT-IR spectra has been used to clarify whether alkaline hydroxides are existing on the surface of Fe_2O_3. FTIR spectrum of pure Fe_2O_3 and KOH/Fe_2O_3 can be seen in fig. 7. The spectra of samples before and after surface modification are approximately similar to each other. The range (3000-3500 cm^{-1}) is mainly related to OH groups [41]. In this range the intensity of the peak has not changed after surface modification.

To investigate the optical properties of alkaline loaded nanoparticles and the pure sample of Fe_2O_3**,** the UV-Visible diffuse reflectance spectroscopy has been used to demonstrate the reflectance and absorbance of samples. In figure 8-a and 8-b reflectance and the absorbance of the used samples of 0.05 wt% KOH/Fe_2O_3 and Fe_2O_3 loaded by 1wt% KOH have been illustrated respectively. For comparison, the spectrum of pure Fe_2O_3 has been indicated. The reflectance of both samples are similar to each other, except for sample with KOH has less value of reflectance than the pure one, this may due to the small change attributed in surface functional groups [27]. Furthermore, the absorbance of samples shows that the edge of absorbance is very similar to each other and it is approximately at the same wavelength. Furthermore, the optical band gap of the pure Fe_2O_3 and KOH loaded Fe_2O_3 was calculated from the Tauc plot in (figure 9) which was derived from a reference [42], and the perfect band gap found to be the direct band gap with values 2.2 eV and 2.25 eV respectively. The observed optical band gap is approximately agreed with published works [16, 18, 33, 43].

To investigate the change in the crystal structure of pure Fe_2O_3 after loaded with KOH, the X-ray diffraction was used. In figure 10, the spectra of pure Fe_2O_3, Fe_2O_3 loaded with KOH and after photoreaction have been shown. One can observe the structure of Fe_2O_3 was crystallized with a monoclinic structure and this result is in a good agreement with the work published [16, 32]. Moreover, other phases of iron oxide are not found in the diffraction peaks and this showed that the impurities are not appeared in the material [32,43]. Then compared spectra of pure one with loaded KOH showed no difference appears in any peaks. That means the crystal structure of Fe_2O_3 was not changed after KOH loading or the quantity of new composition is very low.

According to the results obtained for the photocatalytic activity of samples loaded with alkali hydroxide materials, the reason for the increase of photocatalytic activity should be found in the surface interaction between two materials. We know that metal oxide surfaces are usually covered with hydroxide groups. Two different reactions were proposed for KOH on Fe_2O_3 as below:

$$\mathrm{Fe2O3 + 6\ KOH} \rightleftarrows \mathrm{2\ Fe(OH)3 + 3K2O} \tag{1}$$

$$\mathrm{Fe2O3 + 2\ KOH} \rightleftarrows \mathrm{2\ KFeO2 + H2O(g)} \uparrow \tag{2}$$

According to FTIR spectra in fig. 7 the peaks related to OH groups (3000-3500 cm^{-1}) were not intensified after surface modification. The FTIR spectra shows less OH groups on the surface of Fe_2O_3 due to the modification of KOH on the surface. It shows the first reaction can not be carried out on the surface. The second reaction (2) is mainly happened on the surface and some new nanoparticles are existed on the surface. This is in agreement with the report of L. Khanna et al [41].

By investigating the surface reaction between two materials, it can be supposed that in the single layer of the interface there is an exchange of electrons between the Fe_2O_3 surface and the loaded nanoparticles. Since the alkali nanoparticles are mostly smaller than 20 nm, they can act as cocatalyst material for electron transfer. Actually, it is supposed the connection between iron oxide and alkali nanoparticles causes the photogenerated electrons are transferred from the conduction band of iron oxide to the alkali nanoparticles (fig. 11). It is a routine reported before for different materials [37,38,44].

On the other hand, the photoactivity of iron oxide is low mainly due to the high energy potential of the conduction band in iron oxide (0.2 V vs NHE~) and the low tendency of conduction band to provide electron for one-electron oxygen reduction ($O_2 + H^+ + e^- \longrightarrow HO_2$, -0.046 V). Therefore, one reason may consider for the enhancement of photodegradation is a multi-electron reduction. Two-electron oxygen reduction ($O_2 + 2H^+ + 2e^- \longrightarrow H_2O_2$, +0.68 V and $O_2 + 4H^+ + 4\ e^- \longrightarrow 2H_2O$, +1.23 V vs. NHE pH 0) proceeded over Pt/WO_3 and alkaline/WO_3 has been reported before [39, 45, 46]. It seems reasonable to consider such multi-electron O_2 reduction more readily proceed on the surface of alkaline/Fe_2O_3, compared to the bare surface of Fe_2O_3. Unfortunately, there is not any apparatus to check which mechanism is more probable for this experiment.

4. Conclusion

The loading of very small amounts of alkali metal oxide, such as sodium, potassium, and cesium on the surface of iron (III) oxide particles, increases the photocatalytic activity of iron oxide in the reaction of isopropanol to acetone under visible light irradiation. The results showed that the loaded KOH on Fe_2O_3 surface has improved the most photocatalytic activity compared to other alkaline NaOH and CsOH. Besides, among KOH loaded samples, 0.05 wt% was the desired choice of generated acetone in the photodegradation process. Moreover, for the CO_2 generation the 0.05 wt% loaded KOH sample was the perfect candidate among other samples. XRD spectra showed that the surface of Fe_2O_3 before and after KOH loading had similar crystalized monoclinic structure. Due to the high energy potential of the conductive band in iron oxide and the low tendency of the conduction band to allow the electron to carry out photocatalytic reactions, it can be assumed that the superfacial interaction between the two materials leads to the transfer of photogenerated electrons from iron oxide to alkali nanoparticles on the surface. It results in alkali nanoparticles on the surface act as cocatalyst material (fig. 11). Multi-electron oxygen reduction is another way supposed to facilitate the photocatalytic reaction.

5. Acknowledgment

We would like to express our sincere gratitude and thanks to National Institute for Materials Science (NIMS) specially professor Jinhua Ye who have provided a nice situation for the experiments and study of photocatalytic materials.

6. References

[1] Valle, M. D.; Jurado, E.; Dachs, J.; Sweetman, A. J.; Jones, K. C. *Environ. Pollut.* 2005, *134*, 153-164.

[2] Swearingen, C.; Macha, S.; Fitch, A. *J. Mol. Catal. A: Chem.* 2003, *199*, 149-160.

[3] Rhoton, F. E.; Bigham, J. M.; Lindbo, D. L. *Appl. Geochem.* 2002, *17*, 409-419.

[4] F. B. Li, X. Z. Li, C. S. Liu, X. M. Li and T. X. Liu *Ind. Eng. Chem. Res.* 2007, *46*, 781-787

[5] Mohammad, M.; Syed F. A; Abdullah, Al. *J. S. Chem. So*. 2015, 19 (5), 462-464

[6] Fujishima, A.; Honda, K. *Nature,* 1972, *238*, 37-38.

[7] Linsebigler, A. L.; Lu, G. Q.; Yates, J. T. *Chem. Re*v. 1995, *95*, 735

[8] Jaramillo, T. F.; Baeck, S. H.; Kleiman-Shwarsctein, A.; McFarland, E. W. *Macromol. Rapid Commun.* 2004, *25*, 297.

[9] G.K. Pradhan, D.K. Padhi, K.M. Parida, ACS Appl. Mater. Interfaces. 2013, 5(18), 9101-9110.

[10] Jaramillo, T. F.; Baeck, S. H.; Kleiman-Shwarsctein, A.; Choi, K. S.; Stucky, G. D.; McFarland, E. W. *J. Comb. Chem.* 2005, *7*, 264.

[11] Baeck, S. H.; Choi, K. S.; Jaramillo, T. F.; Stucky, G. D.; McFarland, E. W. *Adv. Mater.* 2003, *15*, 1269.

[12] Baeck, S. H.; Jaramillo, T.; Stucky, G. D.; McFarland, E. W. *Nano Lett.* 2002, *2*, 831.

[13] Su, L. Y.; Zhang, L. G.; Fang, J. H.; Xu, M. H.; Lu, Z. H. *Sol. Energy Mater. Sol. Cells* 1999, *58*, 133.

[14] Gondal, M. A.; Hameed, A.; Yamani, Z. H. *Energy Sources*, 2005, *27*, 1151.

[15] Marsen, B.; Miller, E. L.; Paluselli, D.; Rocheleau, R. E. *Int. J. Hydrogen Energy*, 2007, *32*, 3110.

[16] A. Kleiman-Shwarsctein, Y. S. Hu, A. J. Forman, G. D. Stucky and E. W. McFarland *J. Phys. Chem. C.* 2008, *112*, 15900

[17] T. W. Kim, H. W. Ha, M. J. Paek, S. H. Hyun, I. H. Baek, J. H. Choy and S. J. Hwang *J. Phys. Chem. C.* 2008, *112*, 14853

[18] G. K. Mor, H. E. Prakasam, O. K. Varghese, K. Shankar and C. A. Grimes, *Nano Lett.*, 2007, *7*, 2356.

[19] P. Mallick, B. N. Dash, *Nano. Sci. &Nano tech*. 2013, 3 (5): 130-134

[20] G.K. Pradhan, K.M. Parida, J. Ind. Eng. Chem. 18 (2012) 1612–1619.

[21] G.K. Pradhan, N. Sahu, K.M. Parida, RSC Adv. 3 (2013) 7912–7920.

[22] Ahmed, S. M.; Leduc, J.; Haller, S. F. *J. Phys. Chem.* 1988, *92*, 6655.

[23] G.K. Pradhan, K.M. Parida, Intern. Jour. Engineering, Science and Tech. 2010, 2(9), 53-65.

[24] Itoh, K.; Bockris, J. O. *J. Electrochem. Soc.* 1984, *131*, 1266.

[25] Rosso, K. M.; Smith, D. M. A.; Dupuis, M. *J. Chem. Phys.* 2003, *118*, 6455.

[26] Xu, P.; Zeng, G.M.; Huang, D.L.; Feng, C.L.; Hu, S.; Zhao, M.H.; Lai, C. Z.; Huang, Wei, C.; Xie, G.X.; Liu, Z.F. *Sci. Total Environ*. 2012, 424 ,1–10.

[27] Kako, T.; Meng, X.; Ye, J. *Applied Catal. A, Gen*. 2014, 488, 183–188.

[28] Benjelloun, D.; Bonnet, J. P.; Doumerc, J. P.; Launay, J. C.; Onillon, M.; Hagenmuller, P. *Mater. Chem. Phys.* 1984, *10*, 503.

[29] Morin, F. J. *Phys. Re*v. 1954, *93*, 1195.

[30] Iordanova, N.; Dupuis, M.; Rosso, K. M. *J. Chem. Phys.* 2005, 122.

[31] G.K. Pradhan, K.H. Reddy, K.M. Parida, Catal. Today 224 (2014) 171–179.

[32] Kennedy, J. H.; Frese, J. K. W. *J. Electrochem. Soc*. **1978**, *125*, 709.

[33] Dare-Edwards M., Goodenough J., Hamnett A., Trevellick P. *J. Chem. Soc. Faraday Trans.* 1983, 79, 2027

[34] G.K. Pradhan, K.M. Parida, ASC Apple. Mater. Interfaces, (2011) 317–323.

[35] Kay A.; Cesar I.; Gra¨tzel M., *J. Am. Chem. Soc.* 2006, 128, 15714-15721

[36] Kakuta, S.; Abe, T., *J. Mater. Sci*. 2009, 44, 2890–2898

[37] H. Irie, S. Miura, R. Nakamura, K. Hashimoto *Chem. Lett.* 2008, 37, 252

[38] H. Irie, S. Miura, K. Kamiya and K. Hashimoto, *Chemical Physics Letters* 2008, 457, 202

[39] Khajeh Aminian, M.; Hakimi, M. *Catal. Sci. Technol*.,2014, 4,657–664

[40] Liu, L.; Zachariah, M.R. *Energy Fuels*, 2013, 27, 4977−4983

[41] L. Khanna, N.K. Verma, J. Mater. Sci. Technol., 2014, 30(1), 30-36.

[42] Kumar, V.; Sharma, T.P., *Optical Materials*, 1998, 253–256

[43] Apte, S. K.; Naik, S. D.; Sonawane, R. S.; Kale B. B., *J. Am. Ceram. Soc*., 2007, 412-414.

[44] Khajeh Aminian, M. and Ye, J. *J. Mater. Res.* **2010**, *25*, 141

[45] Abe, R.; Takami, H.; Murakami, N. and Ohtani B. *J. Am. Chem. Soc.*, **2008**, *130*, 7780

[46] M. Khajeh Aminian, N. Taghavinia, A. Irajizad, S.M. Mahdavi, *J. Phys. Chem. C*, **2007**, 111, 9794-9798

Figures

Fig. 1. Acetone generation of Fe_2O_3 under Xe Lamp with 440 nm filter loaded by (a) NaOH (b) KOH (c) CsOH.

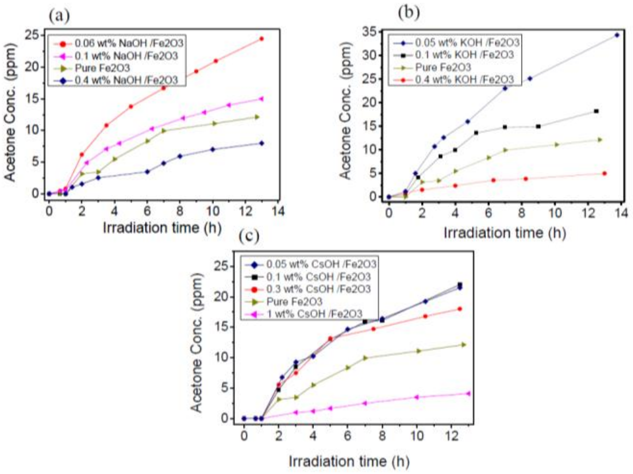

Fig.2.ComparisonofthehighestacetonegenerationonthesurfaceofFe_2O_3thatloadedbyNaOH,KOH,CsOH.

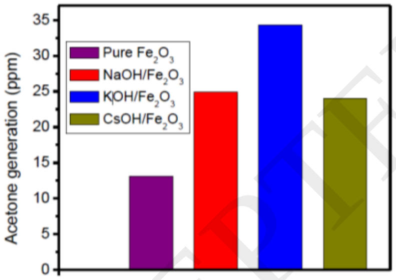

Fig. 3. CO_2 generation under the irradiation of visible light on the process of photodegradation

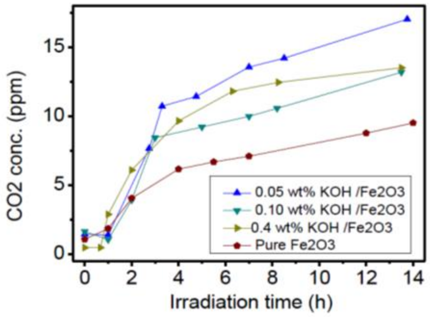

Fig. 4. SEM images of Fe_2O_3loaded by alkaline nanoparticles (a) NaOH(b) KOH (c) CsOH(d) Pure Fe_2O_3.
Average size 106 nm

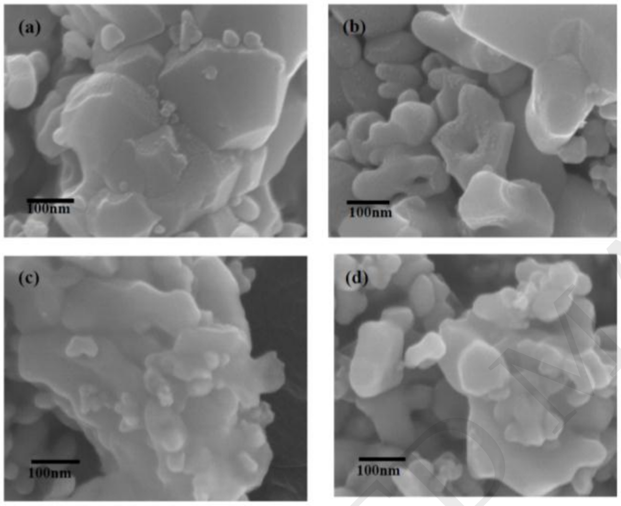

Fig. 5. Particle size histogram of samples from SEM images (a) Fe_2O_3, average size 106 nm (b) KOH/ Fe_2O_3, average size 116 nm

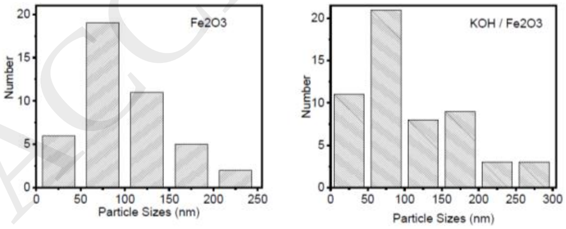

Fig. 6. SEM images of Fe_2O_3loaded by alkaline nanoparticles after photocatalyticreaction (a) NaOH (b) KOH (c) CsOH (d) Pure Fe_2O_3.

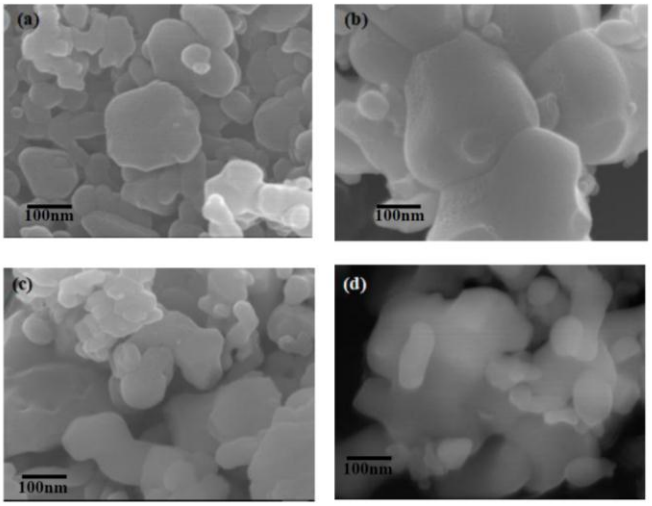

Fig. 7. FTIR spectra shows less OH groups on the surface of Fe_2O_3 due to surface modification by KOH molecules.

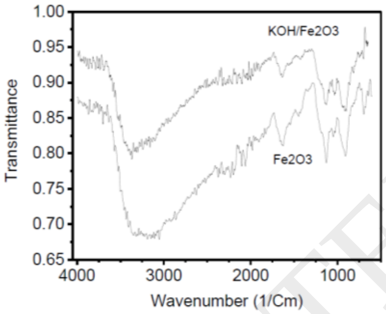

Fig. 8. UV-visible spectroscopy of Fe_2O_3 loaded by KOH. (a) Reflectance and (b) Absorbance

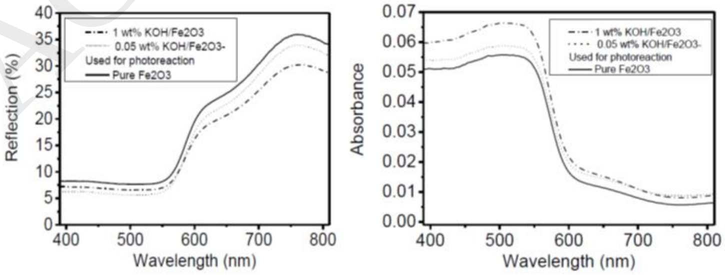

Fig. 9. Bandgap energy of (a) pure Fe_2O_3 2.2 eV and (b) KOH loaded Fe_2O_3 2.25 eV

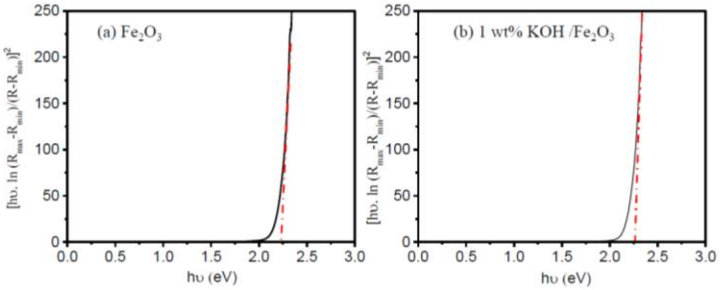

Fig. 10. XRD spectra of pure Fe_2O_3, Fe_2O_3loaded with 1 wt% KOH and the sample used for photocatalyticreaction.

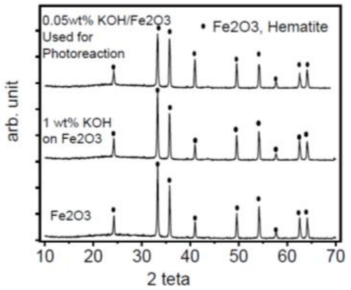

Fig. 11. A Scheme for photocatalyticreaction of IPA on the surface of Fe2O3 modified by alkaline nanoparticles.